THE ASTROPHYSICAL JOURNAL, 446:331–340, 1995 June 10

EINSTEIN OBSERVATIONS OF T TAURI STARS IN TAURUS-AURIGA. I. PROPERTIES OF X-RAY EMISSION

F. DAMIANI, G. MICELA, AND S. SCIORTINO
Istituto ed Osservatorio Astronomico di Palermo, Piazza del Parlamento 1, 90134 Palermo, Italy;
fdamiani, gmicela, ssciortino@oapa.astropa.unipa.it

AND

F. R. HARNDEN, JR.
Harvard-Smithsonian Center for Astrophysics, 60 Garden Street, Cambridge, MA 02138; frh@cfa.harvard.edu
Received 1993 June 15; accepted 1994 December 14

ABSTRACT

We present a systematic reanalysis of the *Einstein* IPC X-ray data on the pre–main-sequence stars in the Taurus-Auriga star formation region. We consider all cataloged stars in this region which have been observed with the IPC; of these, 52 out of 68 can be identified with X-ray sources; upper limits on the X-ray luminosity have been evaluated in the remaining cases. We derive an X-ray luminosity function and argue that its median L_x is representative of the population intrinsic value, in spite of incompleteness of the sample and possible ambiguities in the X-ray source identifications. As a result, it is confirmed that the known steady increase in the average level of X-ray emission toward younger ages can be extended to the pre–main-sequence phase. By using the line equivalent width as the relevant parameter, a statistically significant difference is found between the distributions of X-ray luminosities of stars with and without strong emission lines. No such difference is found instead between stars with and without strong infrared excess at 25 μm.

Subject headings: stars: activity — stars: pre–main-sequence — X-rays: stars

1. INTRODUCTION

Pre–main-sequence (PMS) stars have long been known to exhibit peculiar spectral characteristics at almost all wavelengths with respect to ordinary late-type main-sequence stars (see, e.g., the review by Bertout 1989). Excesses in the line and continuum emission are commonly detected and have therefore been used to identify these stars spectroscopically. Strong emission lines of hydrogen and other elements are usually observed (Cohen & Kuhi 1979), with equivalent widths much above those of dKe–dMe stars, and are well explained by stellar wind models (e.g., Hartmann et al. 1990). In particular, the observations made with the *Einstein Observatory* showed that the emission at X-ray wavelengths of some T Tauri stars is several orders of magnitude enhanced with respect to that of main-sequence stars of similar spectral types, and the same result is currently being obtained from *ROSAT* observations.

In the last 15 years, our knowledge of the X-ray emission from normal stars has increased substantially, mainly on the basis of the data collected with *Einstein* (Vaiana et al. 1981, 1992; Rosner, Golub, & Vaiana 1985; Sciortino 1993, and references therein). It turned out that X-ray emission is detected almost everywhere throughout the H-R diagram, with the possible exception of late B/early A dwarfs and late K and M supergiants. The observed connection between X-ray emission and stellar rotation for late-F to M stars has suggested that a dynamo mechanism gives rise to X-ray emission in these stars, in analogy with the Sun (cf. Rosner & Vaiana 1980).

The average stellar X-ray luminosity of solar-like stars is also known to increase toward younger ages, passing from field stars to the Hyades, Pleiades, and up to the very young PMS stars (Caillault & Helfand 1985; Micela et al. 1985, 1988, 1990; Feigelson & Kriss 1989). In fact, the spatial density of X-ray sources in regions of star formation is higher than the average density over the whole sky since the typical X-ray emission of young stars is high (Montmerle et al. 1983; Feigelson et al. 1987; Walter et al. 1988).

However, systematic studies of X-ray emission are limited to some star formation regions, such as the Chamaeleon region (Feigelson & Kriss 1989) and the Orion B (L1641) cloud (Strom et al. 1990), while for other regions, such as Taurus-Auriga, published papers refer only to subsets of all available data (and were mostly based on early reductions [REV 0] of *Einstein* data). Also, the contribution from *ROSAT* observations of Taurus-Auriga stars is, at present, limited to some star-forming clouds in the region (e.g., L1495E; Strom & Strom 1994).

X-ray observations of small samples of T Tauri stars in Taurus-Auriga have been presented by Gahm (1980), Feigelson & DeCampli (1981), Feigelson & Kriss (1981), and Walter & Kuhi (1981, 1984). A number of stars were detected with the imaging proportional counter (IPC) of the *Einstein* satellite, with X-ray luminosities $L_x \sim 10^{30}$–10^{31} ergs s^{-1}. Since flare-like variability was identified only in a small fraction of the X-ray–detected stars, most of the detected X-ray flux arises from a quiescent component (Feigelson & DeCampli 1981; Walter & Kuhi 1984).

Emission from shocks in circumstellar envelopes is hardly compatible with both the observed X-ray luminosity and typical energies (≥ 1 keV; Feigelson & DeCampli 1981); rather, the rapid variability sometimes observed (Feigelson & DeCampli 1981; Walter & Kuhi 1984; see also Montmerle et al. 1983 about the ρ Oph star-forming region) suggests that the X-ray–emitting regions are fairly small and close to the photosphere. Feigelson & Kriss (1981) argue that this X-ray emission is similar in character to that of main-sequence stars, although scaled up by factors of $\sim 10^3$.

In several star-forming regions, the IPC observations also led to the identification of many new PMS stars, previously

unnoticed due to their weak emission-line activity (Walter & Kuhi 1981; Feigelson & Kriss 1981; Mundt et al. 1983; Walter 1986; Feigelson et al. 1987; Walter et al. 1987, 1988). The studies later than about 1985 made use of the latest revision of IPC data (REV 1), but no reanalysis of the early data on well-known classical T Tauri stars was included, nor was a detailed comparison made between the X-ray properties of the latter and the newly discovered PMS stars.

Therefore, it seemed to us worthwhile to systematically reanalyze the whole *Einstein* X-ray data set provided by the REV 1 release (Harnden et al. 1984), concerning PMS stars in the Taurus-Auriga region (the nearest large star formation region). By considering together stars having widely different levels of activity, we will take advantage of a broader dynamical range, as compared to previous works, over which to study the unclear relationships between the X-ray and line emission in these stars.

The paper is structured as follows: § 2 is a description of the observations, data selection, and data reduction; in § 3 the average X-ray properties of various subsamples are tested by the use of X-ray luminosity functions; the main results obtained are summarized in § 4.

2. DATA SELECTION AND ANALYSIS

2.1. *Observed Sample*

Our sample is composed of all PMS stars in the Taurus-Auriga star formation region which are listed in the Herbig & Bell (1988) catalog of emission-line stars of the Orion population (hereafter HBC) and which have been observed in X-rays with the *Einstein Observatory*. The HBC is an update of the Herbig & Rao (1972) catalog, and most of the new catalog entries are stars which exhibit a general activity far less intense than classical T Tauri stars (CTTSs) and which have been named weak-lined T Tauri stars (WTTSs). Due to the different techniques used in selecting various classes of stars, the homogeneity and completeness of the catalog is not guaranteed, as explicitly stated by the authors themselves. Most WTTSs have been selected as PMS stars as a result of searches for emission in the Ca II H and K lines (Herbig, Vrba, & Rydgren 1986) or for strong X-ray sources in regions of stellar formation (Walter 1986; Walter et al. 1988), and our WTTS sample is therefore biased toward bright X-ray sources. We have, however, attempted to build an *unbiased* WTTS sample made of all WTTSs not originally selected as X-ray sources, and we have compared results obtained from this small subsample with those derived for the whole WTTS sample.

Due to the difficulty of distinguishing a star near the end of its PMS phase (or with low line emission anyway) from a very young main-sequence star, and since possible main-sequence stars have been conservatively excluded from the HBC, the catalog should be quite incomplete for stars in their latest PMS stages. Indeed, despite the variety of techniques used to find stars in this evolutionary stage, the known stars with estimated ages of $\sim 10^7$ yr have remained much less numerous than expected (Kenyon & Hartmann 1990; Herbig et al. 1986).

In this respect we note that recently Favata et al. (1993), analyzing the lithium abundance in a sample of G and K coronal sources selected from the X-ray flux limited Extended Medium Sensitivity Survey (Gioia et al. 1990; Stocke et al. 1991), have shown that a sizeable fraction of high-latitude ($|b| > 20°$) coronal sources outside of "classical" star formation regions are indeed young or PMS stars.

We define the Taurus-Auriga region as the sky region within $3^h0^m0^s <$ R.A. $< 5^h5^m0^s$ and $+15° <$ decl. $< +40°$; 160 HBC stars fall inside this region[1] (Fig. 1). They are distributed highly nonuniformly across the region, except for the WTTSs, which, as already noted by Walter et al. (1988), generally keep at a greater distance from the cloud center.

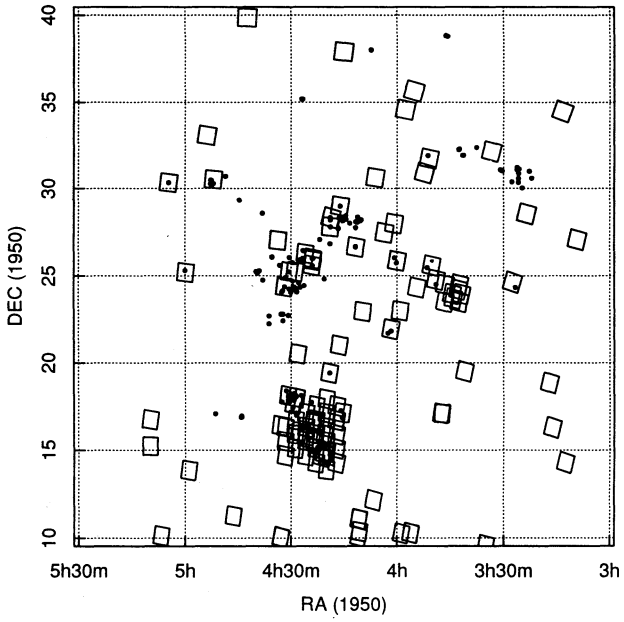

FIG. 1.—Spatial map of the sky region of Taurus-Auriga. All stars of the optical parent sample are shown as dots, and the squares represent the *Einstein* IPC fields of view in this region.

From the previously defined sample we have extracted all stars which have been observed in X-rays with the *Einstein Observatory* (Giacconi et al. 1979); the IPC (Gorenstein, Harnden, & Fabricant 1981) was the only instrument on this satellite which observed stars of our sample, in the energy band 0.16–3.5 keV.

It is worthwhile to note how a certain degree of inhomogeneity in the optical sample, containing stars selected in various ways (Hα, Ca II, X-ray emission), affects our study of X-ray emission properties: Stars selected through Hα (or Ca II H and K) emission are an unbiased sample with respect to X-ray emission. This is not true for X-ray–selected stars, which constitute most of known WTTSs, as noted, and for which the L_x distribution we derive may describe, in principle, only the high-L_x tail of their true distribution. However, the existence of a large number of unknown WTTSs below our detection threshold is not suggested by the L_x distribution of WTTSs selected independent of X-rays (see § 3.1). A caveat is in order, in any case, since this latter sample may not be entirely unbiased with respect to X-rays: in fact, these stars were selected on the basis of their Hα or Ca II emission, which are shown to correlate with X-ray emission in the case of WTTSs, as we discuss in a companion paper (Damiani & Micela 1995, hereafter Paper II).

In Figure 1 we show all the IPC fields in the Taurus region (*squares*), together with all PMS stars of the optical sample (*dots*); it is seen that only a small fraction of the region is covered by the X-ray observations. In total, 71 stars of our optical sample, contained in 34 distinct IPC fields, have been observed by *Einstein*. We have verified that the distribution of

[1] We have however excluded from the sample the star Wa Tau/1 (HBC 408), since this was not considered a PMS star by Walter (1986).

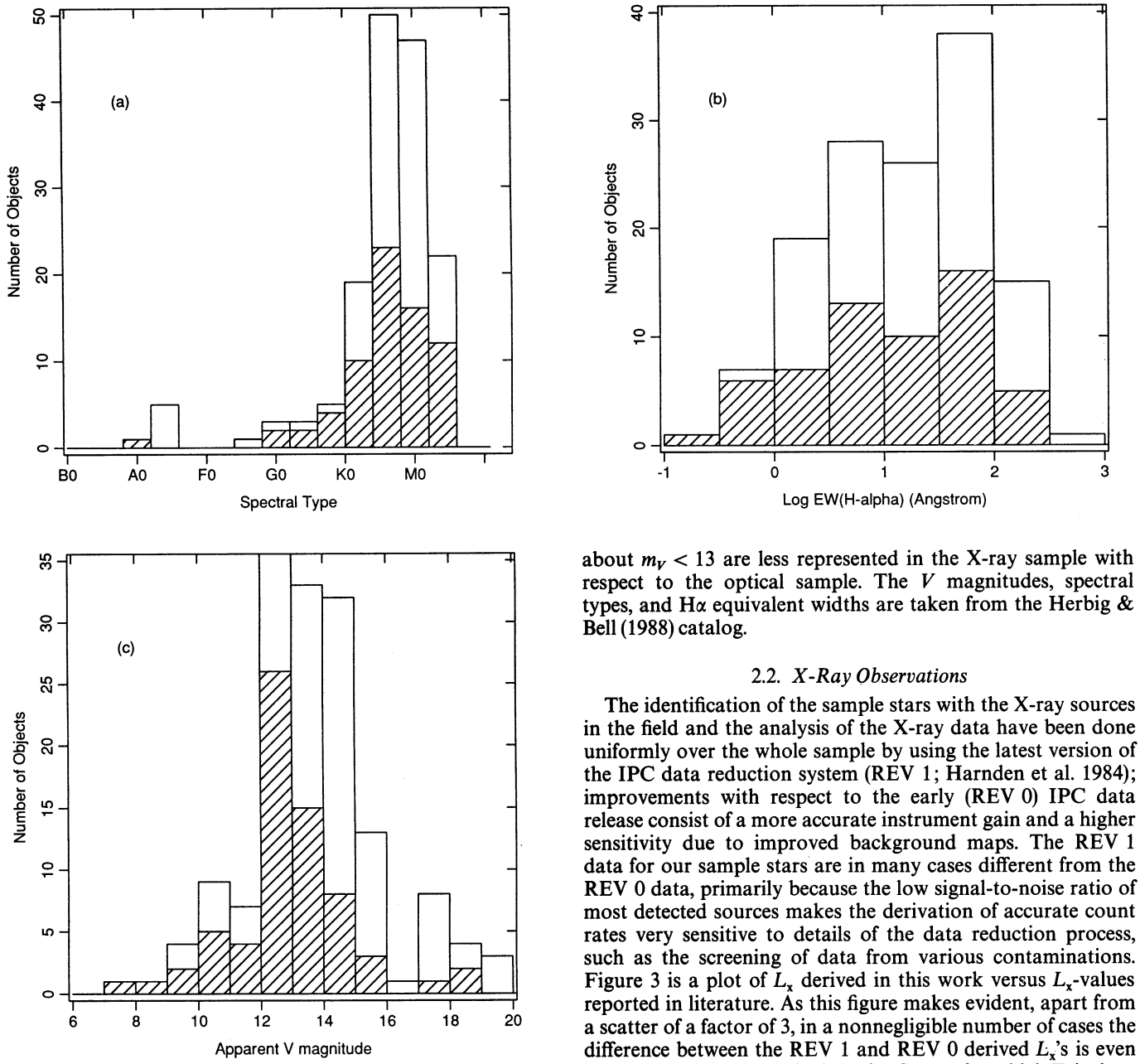

FIG. 2.—Distributions of spectral types (*a*), Hα equivalent width (*b*), and apparent V magnitude (*c*) for the stars in the optical sample (*blank bins*) and in the X-ray sample (*hatched bins*).

spectral types in this sample is nearly identical to that of the optical sample and, therefore, is not affected by the incomplete sampling of the X-ray observations (Fig. 2*a*) (a Pearson's χ^2 test [Eadie et al. 1971] applied to the two distributions gives a probability of only $P = 17\%$ of not being drawn from the same parent population). The same holds for the distribution of levels of atmospheric activity, as indicated by the Hα line equivalent width (Fig. 2*b*), with a χ^2 test probability of $P = 24\%$. A comparison of the visual magnitude distributions of the optical and X-ray samples gives instead some indication that these distributions may be different with a probability of $P = 95\%$. A visual inspection of the two distributions (Fig. 2*c*) suggests that this difference arises because stars fainter than about $m_V < 13$ are less represented in the X-ray sample with respect to the optical sample. The V magnitudes, spectral types, and Hα equivalent widths are taken from the Herbig & Bell (1988) catalog.

2.2. *X-Ray Observations*

The identification of the sample stars with the X-ray sources in the field and the analysis of the X-ray data have been done uniformly over the whole sample by using the latest version of the IPC data reduction system (REV 1; Harnden et al. 1984); improvements with respect to the early (REV 0) IPC data release consist of a more accurate instrument gain and a higher sensitivity due to improved background maps. The REV 1 data for our sample stars are in many cases different from the REV 0 data, primarily because the low signal-to-noise ratio of most detected sources makes the derivation of accurate count rates very sensitive to details of the data reduction process, such as the screening of data from various contaminations. Figure 3 is a plot of L_x derived in this work versus L_x-values reported in literature. As this figure makes evident, apart from a scatter of a factor of 3, in a nonnegligible number of cases the difference between the REV 1 and REV 0 derived L_x's is even larger. An extreme case is that of DG Tau, for which Feigelson & DeCampli (1981) reported a large X-ray flare, while REV 1 data of the same IPC observation do not even show a source at that stellar position, but only a constant X-ray background. We have therefore chosen to carry out the X-ray data analysis for these stars independent of previously published work. In particular, the homogeneous data reduction procedure for both CTTSs and WTTSs allows a careful comparison of their respective X-ray properties.

The REV 1 system uses two distinct methods to detect X-ray sources in each image, namely, the "Map" and "Local" methods (differing in the evaluation of the X-ray background; see, e.g., Micela et al. 1988), each one applied in the "soft" (0.16–0.8 keV), "hard" (0.8–3.5 keV), and "broad" (0.16–3.5 keV) IPC spectral bands.

The spatial resolution varies with observed pulse height, but is always better than 3′. We have cross-checked the optical

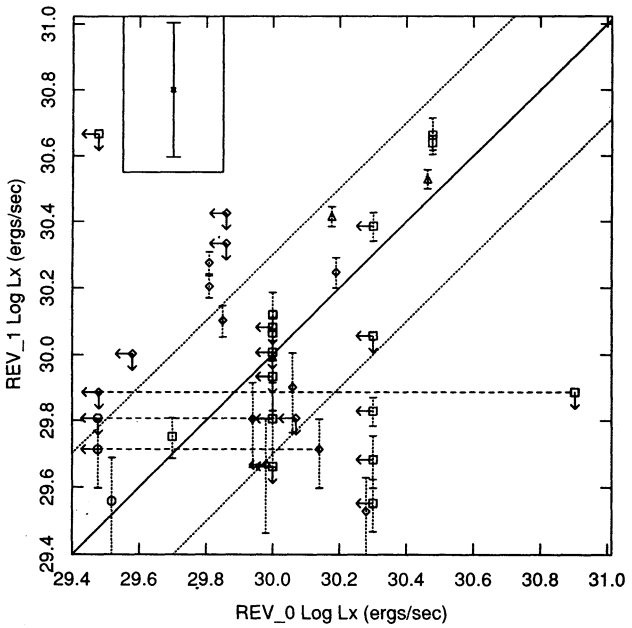

FIG. 3.—Comparison of L_x derived in this work, using REV 1 IPC data, with those published in literature, based on REV 0 data. The various symbols refer to Gahm (1980, *circles*), Feigelson & Kriss (1981, *triangles*), Feigelson & DeCampli (1981, *squares*), and Walter & Kuhi (1981, *diamonds*). Dashed segments connect different published L_x values for a given star. The solid line represents identity, and dotted straight lines represent a factor of 2 difference between REV 0 and REV 1 L_x's. Error bars for REV 1 data (*dotted*) refer to statistical uncertainties alone; the typical overall uncertainty in L_x, mostly due to the absorption correction, is shown as the bar in the box in the upper left of the figure. Note that, given the size of the systematic uncertainties, differences between REV 0 and REV 1 L_x's greater than a factor of 2 are significant.

positions of all stars in the X-ray sample with the positions of all X-ray sources in Taurus-Auriga. We found that 53 stars fall within (3′ radius) circles centered on X-ray sources, corresponding to 38 distinct X-ray sources (16 out of these 38 sources are observed more than once). In 24 cases there is a single star of our sample within 3′ of the corresponding X-ray source: we shall occasionally refer to these stars as "single identifications." In addition, we found 13 pairs and a group of three stars of the sample within 3′ of the corresponding X-ray sources ("multiple identifications"); these are the pairs RY Tau/LkCa 21, DH/DI Tau, UX Tau A/B, V710 Tau A/B, GH/V807 Tau, GI/GK Tau, AB/SU Aur, RW Aur A/B, NTTS 035120+3154 SW/NE, NTTS 035135+2528 NW/SE, NTTS 040012+2545 S/N, NTTS 040047+2603 W/E, NTTS 040142+2150 SW/NE, and the group HL Tau, XZ Tau, and LkHα 358. In these cases the IPC data alone cannot indicate what fraction of the observed counts is contributed from each star.

In one case it seemed possible to refine the identification made. The stars AB Aur and SU Aur are identified with the same X-ray source, and their offsets between X-ray and optical positions are ∼2.″7 and ∼0.″3, respectively. Therefore, also taking into account their small off-axis position in the IPC image and the large number of recorded X-ray photons, which reduces the positional error, we have identified uniquely the X-ray source with SU Aur, treating AB Aur as not detected in X-rays. This reduces the number of stars having an X-ray counterpart more distant than 1′ to only two. We then obtain that, out of 71 stars observed in X-rays by *Einstein*, 52 are identified with X-ray sources, and we have evaluated upper limits to the X-ray luminosity of the remaining 19 stars.

The standard IPC data reduction system gives, for each detected X-ray source (for each detection method and spectral band), the value of the background-corrected recorded count rate (Harnden et al. 1984). To preserve maximum uniformity in the data analysis of our whole sample, we have chosen to use the data obtained with the Map method in the broadband, which detects the greatest number of objects in our sample; only three objects are detected exclusively by the Local method, or by the Map method in other spectral bands. In these latter three cases, we used count rates given by the Local method, in the same broad energy band.

For optical stars observed and detected in more than one IPC field (16 distinct X-ray sources in our sample), we have chosen to ignore those detections affected by the detector-supporting structure and edges, since they are of much poorer quality. This procedure results in a single count rate for the X-ray source identified with each star, except for five stars: three of these are single identifications, and the remaining pair is identified with a single X-ray object, so in total we have four X-ray objects, each observed twice. In these cases we have chosen to adopt a "maximum likelihood" procedure (Sciortino & Micela 1992) to assign a single count rate to each given X-ray object (obtained as a weighted mean, according to the statistical errors, of the values given by each observation).[2]

The count rates can be transformed into observed fluxes (between 0.16 and 3.5 keV) using a conversion factor (Harris et al. 1993), computed for the IPC broadband by assuming a Raymond thermal spectrum (Raymond & Smith 1977), and depending on the source temperature and on the line-of-sight hydrogen column density N_H. Taking advantage of the spectral resolution of the IPC, one can define the hardness ratio (HR) as

$$\mathrm{HR} = \frac{\text{counts(hard band)} - \text{counts(soft band)}}{\text{counts(hard band)} + \text{counts(soft band)}}.$$

Hardness ratios for our X-ray sources are generally quite higher than those observed for main-sequence stars, in agreement with previous work (Feigelson & Kriss 1981; Walter & Kuhi 1981, 1984), apparently indicating quite high temperatures for the X-ray–emitting plasma of PMS stars. However, since these HRs are in most cases affected by large errors, they cannot be reliably used to deduce temperature values. We have instead performed spectral fits on the two sample stars with the largest number of X-ray counts (SU Aur and HD 283572) using the IRAF/PROS spectral package, which yielded temperatures of 1.1 (1.0–1.5) keV and 1.5 (1.1–2.3) keV, respectively; the result for HD 283572 is compatible with the value of 2.2 (1.1 to >15) keV reported by Schrijver, Mewe, & Walter (1984), as well as with the detailed analysis of the X-ray spectrum of this star made by Walter et al. (1987). The mean of the two temperatures we derive (1.3 keV, corresponding to $T = 1.5 \times 10^7$ K) is compatible with the HR observed for the other sample stars, and therefore we have assumed this temperature for all stars of the sample. For T

[2] The validity of the procedure may be questioned if the individual values of the count rate differ beyond the 3 σ value, because this would indicate intrinsic X-ray variability. This happens only for AA Tau among the objects considered here, detected twice with count rates of 0.024 ± 0.005 and 0.005 ± 0.001 counts s^{-1}, respectively. However, since we lack details of its X-ray light curve, we have applied the maximum likelihood procedure even in this case. There is no clear evidence that the larger X-ray count rate has to be ascribed to a large flare, since the X-ray light curve at X-ray maximum, as derived by us from REV 1 data, is flat over the observation time span of 2032 s. Of course, further studies on the nature of X-ray variability in T Tauri stars are warranted.

higher (lower) by a factor of 2, the error in the conversion factor would be +13.8% (−8.9%) for a typical $N_H = 1.4 \times 10^{21}$ cm^{-2} and −16.2% (+105.0%) for a quite extreme value of $N_H = 7.7 \times 10^{21}$ cm^{-2}. The value of N_H is estimated for the individual stars from the optical extinction A_V, assuming for the entire line of sight a mass ratio between neutral hydrogen and dust equal to the average interstellar ratio, and making use of the relation $N_H = 2.22 \times 10^{21} A_V$ cm^{-2} (Gorenstein 1975). The values for the optical extinction are taken from Cohen & Kuhi (1979) and Strom et al. (1989). An error by a factor of 2 higher (lower) in the value of N_H about the estimated values, and for the temperature range of our interest, results in an error in the conversion factor of +35.0% (−16.1%). For the stars without a published extinction value we adopted an average conversion factor of 3.41×10^{-11} ergs cm^{-2} count^{-1} (corresponding to $N_H = 1.4 \times 10^{21}$ cm^{-2}). The evaluation of uncertainties on the values of N_H is difficult, not only because A_V-values from different authors may easily differ by ∼1 mag, but also since the adopted proportionality between N_H and A_V might not hold in a T Tauri star circumstellar environment. For example, a hot, dust-free wind will contribute only to N_H, but not to the optical extinction A_V. Using N_H as given by X-ray spectral fits on HD 283572 and SU Aur we derive N_H/A_V ratios of 9.6 (6.1–27.2) $\times 10^{20}$ and 6.9(3.4–7.6) $\times 10^{21}$ cm^{-2} mag^{-1}, respectively, which bracket the interstellar value and are compatible with it to within the 3 σ level. The reliability of the absorption corrections we have applied will also be discussed in Paper II in connection with the correlations of X-ray emission with stellar properties.

Assuming all stars to be at the distance of the Taurus-Auriga complex (140 pc), we then obtain a value of L_x for each source. Given the sky-projected extension of the cluster (∼20 pc) we estimate an error of 14% in L_x, on the basis of the lack of individual distance values alone. Taking into account all sources of uncertainty, the typical overall uncertainty in L_x is 55% (rising to 65% for the lowest signal-to-noise detections) and is mainly due to the poor knowledge of N_H (and A_V).

In the case of multiple identifications, we have divided equally the observed counts between the optical counterparts. This approach gives maximum likelihood X-ray luminosities, if we lack a valid criterion to split the observed count rate among counterparts. Since we will present in Paper II various dependences of L_x on bolometric luminosity, rotation rate, and Hα emission (holding for various subsamples), it is not clear which criterion should be applied in each case. This is a fundamental problem with all low spatial resolution detectors and cannot be solved until higher resolution observations are available. Since it affects about half our sample, we will treat single identifications distinctly from multiple identifications to check the extent to which the identification problem affects the correlations found (Paper II).

Alternatively, since Walter et al. (1988) found that the X-ray surface flux is roughly constant during the PMS phase, one could split count rates in proportion to the squared stellar radii, or to bolometric luminosities. This approach would yield L_x-values significantly different from those we have derived only for a few stellar pairs whose components are quite different, such as RW Aur A/B or UX Tau A/B. For these cases, the X-ray luminosity of the primary would increase by a factor of 2 with respect to the value we have derived. Given the overall uncertainty in L_x, this would not sensibly affect any of our conclusions.

2.3. *Undetected Stars*

In addition to the stars identified with X-ray sources, we also consider those observed by the IPC but undetected in X-rays in any band by any method. There are 19 such stars in our sample. However, three of them fell behind detector ribs and were therefore discarded from our sample as not having been observed. Among these, the star HBC 412 deserves special mention: this star falls ∼2.3 from *two* distinct X-ray detections *in the same IPC image*. Because these sources are only detected with the Map method, are quite far (∼30′) from the telescope axis, and are strongly obscured by the detector ribs, we could not derive even an approximate X-ray count rate for this star, and we have omitted it altogether from our sample, despite its likelihood of being an X-ray emitter. We are thus left with 16 stars for which we calculate an upper limit to L_x. We have followed the prescriptions of Harris et al. (1993), which allow us to obtain 3.5 σ limiting count-rate values, knowing the star position relative to a specific IPC image and the exposure time of the latter.

Once an upper limit to the recorded count rate was obtained in this way for each undetected star, we proceeded as for detections to get a limiting value for L_x, using a value of N_H derived from A_V and assuming the same temperature as adopted for detections. The X-ray data for all stars in the observed sample are summarized in Tables 1A and 1B, together with other relevant data taken from literature. The quantity η, whose correlation with L_x is extensively discussed in Paper II, is reported here for completeness.

3. RESULTS AND DISCUSSION

3.1. *Level of X-Ray Emission in Taurus-Auriga*

We have analyzed the X-ray data obtained for the Taurus-Auriga T Tauri stars by computing maximum likelihood X-ray luminosity functions, a method often employed to examine distributions of quantities including upper limits and therefore well suited to our X-ray data (see Avni et al. 1980; Schmitt 1985; Feigelson & Nelson 1985). The X-ray luminosity function for our stars is shown as the solid line in Figure 4; we see that L_x ranges from $10^{29.5}$ to $10^{31.4}$ ergs s^{-1}, with the lower value set by the instrument sensitivity threshold. The median of log L_x is $29.82^{+0.08}_{-0.06}$, and its mean is 29.91 ± 0.04, where the 1 σ errors were computed using a "bootstrap" procedure with 200 iterations (cf. Schmitt 1985). Having detected as X-ray sources *at least* 38 stars out of 68 (this number is obtained by considering as detected only one star for each multiple identification), the measured median L_x for our sample is at first sight representative of the entire Taurus-Auriga PMS population; however, this might be a result of the sample composition.

If we restrict ourselves to the group of CTTSs alone, we detect at least 17 (and up to 26) stars out of 42 (the ambiguity is again due to the problem of multiple identifications). Here we separate CTTSs from WTTSs on the basis of their detection at 25 μm, which is a better proxy than Hα emission to sample circumstellar activity. With the percentage of detections ranging from 40% to 62%, we are not entirely sure of having reached the median, whose true value might therefore be slightly lower than the one we calculate (median log L_x = 29.74 [ergs s^{-1}]) for the CTTSs alone. On the other hand, in the case of the WTTSs we have 81%–100% detected stars, which is simply a result of the sample composition; therefore, in this case also the true median X-ray luminosity is likely to be lower than the obtained value of median log L_x = 29.93 (ergs

TABLE 1A

SUMMARY OF DATA FOR X-RAY–DETECTED T TAURI STARS

HBC No.	Name	IPC Sequence	t_{exp} (s)	Count Rate (counts s^{-1})	S/N	A_V[a]	log L_x (erg s^{-1})	m_v[b]	Spectral[b] Type	EW(Hα)[b] (Å)	P_{rot} (days)	Ref.	log L_{bol} ($L_\odot$)	Ref.	log $L_{H\alpha}$[c] (erg s^{-1})	log $L_{25\mu m}$[d] (erg s^{-1})	log age (yr)	log η
32	BP Tau	4514	2679	0.009	3.7	0.84	29.90	12.09	K7	40	7.6	2	0.13	3	31.11	32.05	5.57	-0.95
34	RY Tau	4507	2247	0.014	4.3	0.55	29.71	10.01	K1	20	6.54	4	0.99	3	31.48	33.72	5.73	-2.24
35[e]	T Tau	3816	2666	0.035	7.9	1.67	30.66	9.90	K0	60	2.8	5	0.85	3	32.37	33.94	5.95	-1.58
		7434	1916	0.048	...	...	...	...	...	...	...	...	...	...	...	...	...	...
36	DF Tau	10573	3529	0.009	3.5	0.55	29.81	11.49	M0	60	8.5	6	0.78	3	31.40	32.35	4.75	-0.95
38	DH Tau	3818	2664	0.025	6.0	1.52	30.12	13.92	M1	53	7	7	-0.21	3	30.80	31.85	5.71	-1.05
39	DI Tau	3818	2664	0.025	6.0	1.08	30.07	12.86	M0	2	7.7	7	0.09	3	29.65	31.63	5.61	-1.98
42	UX Tau B	7247	10563	0.052	16.1	0.57	30.29	13.67	M1	4	...	...	-0.46	3	29.47	...	6.08	...
43	UX Tau A	7247	10563	0.052	16.1	0.47	30.26	10.69	K2	3.9	2.7	8	0.03	3	30.58	32.51	6.87	-1.93
49	HL Tau	7247	10563	0.018	10.1	0.65[f]	30.39	14.57	K7	55	...	...	0.64	9	32.13	33.71	4.75	-1.58
50	XZ Tau	7247	10563	0.018	10.1	1.71	29.83	13.30	M3	274	...	...	0.66	3	31.70	33.08	4.74	-1.38
51	V710 Tau A	7247	10563	0.008	5.7	1.80	29.68	13.65	M1	48	...	...	-0.59	3	30.98	31.94	6.22	-0.96
55	GH Tau	4516	1965	0.015	2.7	0.25	29.67	12.95	M2	15	...	...	0.06	3	30.24	32.26	5.54	-2.02
56	GI Tau	10069	9511	0.038	13.1	1.33	30.28	13.01	K6	19	7.2	10	0.12	3	30.66	32.47	5.66	-1.81
57	GK Tau	10069	9511	0.038	13.1	0.78	30.20	12.14	K7	16	4.6	10	0.19	3	30.84	32.47	5.52	-1.63
63[e]	AA Tau	4516	1965	0.023	3.9	0.84	29.53	12.37	K7	37	8.2	7	0.02	3	30.96	32.04	5.65	-1.08
		10069	9511	0.005[g]	...	...	...	...	...	...	...	...	...	...	...	...	...	...
65	DN Tau	10069	9511	0.019	9.3	0.35	30.10	12.36	M0	12	6	8	0.17	3	30.53	32.09	4.88	-1.56
77	GM Aur	3810	11156	0.010	7.1	0.10	29.75	12.03	K3	96	12.0	18	0.05	3	31.28	32.32	6.58	-1.04
79	SU Aur	3810	11156	0.056	19.8	0.64	30.64	8.93	G2	4	2.73	11	1.12	3	31.17	33.40	6.35	-2.23
80	RW Aur A	3841	1880	0.008	2.9	0.65[f]	29.56	10.12	K1	84	5	12	0.74	9	32.24	32.85	5.99	-0.61
81	RW Aur B	3841	1880	0.008	2.9	0.65[f]	29.56	12.70	K3	...	...	...	-0.26	1	...	...	7.14	...
347	032641+2420	3440	2082	0.013	3.3	0.30	29.94	12.05	K1	...	...	...	-0.30	13	29.39	<31.09	7.44	...
351	034903+2431	3175	1313	0.022	3.8	0.04	30.05	12.26	K5	1.6	$\leq$3.5	18	-0.30	13	29.64	<30.95	6.71	...
352	035120+3154SW	2227	2882	0.013	4.3	0.91	29.76	11.85	G0	...	...	...	-0.11	13	29.19	<30.85	7.50	...
353	035120+3154NE	2227	2882	0.013	4.3	1.03	29.78	12.31	G5	...	...	...	-0.24	13	28.79	<30.85	7.57	...
354	035135+2528NW	7408	2421	0.012	3.4	0.61	29.67	13.79	K3	...	...	...	-0.65	13	28.74	<30.85	7.53	...
355	035135+2528SE	7408	2421	0.012	3.4	0.15	29.55	12.67	K0	...	...	...	-0.51	13	28.74	<30.85	7.69	...
356	040012+2545S	7164	1978	0.011	3.2	0.65[f]	29.65	12.91	...	0.9	...	...	-0.78	13	28.19	<30.85	...	...
357	040012+2545N	7164	1978	0.011	3.2	0.61	29.63	12.91	K2	1.8	...	...	-0.78	13	28.19	<30.85	7.92	...
358[e]	040047+2603W	3994	2283	0.027	2.9	0.68	29.89	14.52	M2	7.8	...	...	-0.47	13	29.79	<30.85	5.93	...
		7164	1978	0.011	...	...	...	...	...	...	...	...	...	...	...	...	...	...
359[e]	040047+2603E	3994	2283	0.027	2.9	0.42	29.82	14.17	M2	2.4	...	...	-0.56	13	29.38	<30.85	6.03	...
		7164	1978	0.011	...	...	...	...	...	...	...	...	...	...	...	...	...	...
360	040142+2150SW	7918	3565	0.050	10.8	1.10	30.37	14.97	M3	7.6	...	...	-0.60	13	29.34	...	5.98	...
361	040142+2150NE	7918	3565	0.050	10.8	0.61	30.28	15.09	M3	5.7	...	...	-0.76	13	29.17	...	6.11	...
362	040234+2143	7918	3565	0.007	3.0	0.38	29.68	14.67	M2	4	...	...	-0.70	13	29.37	<30.85	6.20	...
372	041529+1652	9000	9132	0.006	4.6	0.00	29.48	13.26	K5	...	...	...	-0.75	13	28.27	<30.95	7.68	...
376	041559+1716	9000	9132	0.020	10.0	0.00	29.98	12.28	K7	0.7	...	...	-0.32	13	29.47	<30.95	6.31	...
379	041636+2743	3843	2066	0.021	3.6	0.76	30.25	12.37	K7	4	5.64	18	-0.01	13	29.94	<30.85	5.68	...
380	HD 283572	4507	2247	0.336	22.6	0.57	31.40	9.04	G5	...	1.548	14	0.84	13	...	<31.53	6.58	...
382	LkCa 21	4507	2247	0.014	4.3	0.65[f]	29.74	13.50	M3	6	...	...	0.25[h]	18	30.41	32.21	4.75	-1.80
388	042417+1744	3528	4005	0.069	10.8	0.00	30.52	10.34	K1	...	...	...	0.22	13	29.74	<30.85	6.70	...
392	042835+1700	3526	1935	0.017	3.8	0.15	29.99	12.53	K5	0.2	3.38	18	-0.37	13	29.17	<30.85	6.81	...
394	LkHα 358	7247	10563	0.018	10.1	0.65[f]	29.59	19.00	M5.5	47	...	...	-2.80	9	28.13	...	8.00	...
395	V710 Tau B	7247	10563	0.008	5.7	0.65[f]	29.55	14.60	M3	3.3	...	...	-0.46	3	29.74	...	5.40	...
397[e]	042916+1751	867	2054	0.013	3.5	0.00	29.91	12.06	K7	0.5	1.21	18	-0.18	13	29.44	<30.95	5.97	...
		7247	10563	0.017	...	...	...	...	...	...	...	...	...	...	...	...	...	...

TABLE 1A—*Continued*

HBC No.	Name	IPC Sequence	t_{exp} (s)	Count Rate (counts s^{-1})	S/N	A_V[a]	log L_x (erg s^{-1})	m_v[b]	Spectral[b] Type	EW(Hα)[b] (Å)	P_{rot} (days)	Ref.	log L_{bol} ($L_\odot$)	Ref.	log $L_{H\alpha}$[c] (erg s^{-1})	log $L_{25\mu m}$[d] (erg s^{-1})	log age (yr)	log η
399	V827 Tau	7247	10563	0.044	15.0	0.61	30.53	12.18	K7	1.8	3.63	15	0.04	13	30.03	<31.15	5.65	...
400	V826 Tau	7247	10563	0.036	14.5	0.53	30.42	12.11	K7	1.6	4.05	15	-0.30	13	29.27	<31.15	6.09	...
403	042950+1757	3819	2644	0.016	4.3	0.91	30.15	13.22	K7	0.7	...	...	-0.36	13	29.49	<30.85	6.33	...
404	V807 Tau	4516	1965	0.015	2.7	0.65[f]	29.55	11.22	K7	13	...	...	-0.12[h]	19	30.53	...	5.90	...
405	V830 Tau	10069	9511	0.026	9.6	0.42	30.25	12.21	K7	3	2.76	15	-0.05	13	29.79	<31.20	5.70	...
407	043124+1824	3819	2644	0.009	2.8	1.22	29.93	12.67	G8	...	...	...	-0.30	13	29.19	<30.85	7.63	...
426	LkCa 19	3810	11156	0.013	8.1	0.65[f]	29.81	10.85	K0	1	2.24	18	0.20	13	29.95	<31.09	6.81	...
427	045251+3016	3810	11156	0.026	11.8	0.00	30.10	11.60	K7	0.7	4.70	18	0.01	13	29.73	31.72	5.67	-2.00
429	V836 Tau	2684	1697	0.011	3.2	0.91	29.99	13.13	K7	9	6.99	15	-0.15	13	30.14	31.61	5.95	-1.47

TABLE 1B

SUMMARY OF DATA FOR T TAURI STARS WITH X-RAY UPPER LIMITS

HBC No.	Name	IPC Sequence	t_{exp} (s)	Count Rate (counts s^{-1})	A_V[a]	log L_x (erg s^{-1})	m_v[b]	Spectral[b] Type	EW(Hα)[b] (Å)	P_{rot} (days)	Ref.	log L_{bol} ($L_\odot$)	Ref.	log $L_{H\alpha}$[c] (erg s^{-1})	log $L_{25\mu m}$[d] (erg s^{-1})	log age (yr)	log η
26	FP Tau	3815	1571	<0.013	0.26	<29.93	13.9	M4	38	...	...	-0.27	3	30.30	31.68	5.00	-1.38
27	CX Tau	3815	1571	<0.014	0.85	<30.08	13.72	M2.5	20	...	...	-0.17	3	30.25	31.85	4.75	-1.60
33	DE Tau	3843	2066	<0.010	0.20	<29.81	13	M2	54	7.6	18	-0.14	3	30.77	32.15	4.75	-1.38
37	DG Tau	10573	3529	<0.008	1.28[i]	<29.89	12.01	M	113	6.3	18	0.88	9	31.71	33.62	4.75	-1.91
41	IQ Tau	3818	2664	<0.012	0.77	<30.01	13.3	M0.5	7.8	...	...	-0.18	3	29.98	32.13	5.82	-2.15
52	UZ Tau e	4515	1986	<0.025	0.85	<30.33	12.86	M1	82	...	...	-0.07	3	31.44	32.53	5.59	-1.09
53	UZ Tau w	4515	1986	<0.025	1.53	<30.43	14.6	M3	80	...	...	-0.38	3	31.31	...	5.18	...
54	GG Tau	867	2054	<0.013	0.78	<30.04	12.24	K7	54	10.3	18	0.12	3	31.22	32.53	5.58	-1.31
58	DL Tau	4515	1986	<0.010	1.28[i]	<30.00	13.05	K7	105	9.4	18	0.17	9	31.31	32.43	5.54	-1.12
60	HN Tau	867	2054	<0.015	0.54	<30.06	13.7	K5	139	...	...	-0.48	3	30.93	32.55	7.09	-1.62
62	DM Tau	10538	2614	<0.010	0.00	<29.66	13.99	M1	139	...	...	-0.77	3	30.70	31.82	6.77	-1.11
78	AB Aur	3810	11156	<0.056	0.65	<30.64	7.07	B9	27	1.88	17	1.78	3	32.65	...	6.56	...
386	FV Tau	10572	3327	<0.008	4.83	<29.69	15.4	K5	23	...	...	0.41	3	31.32	32.78	5.49	-1.45
387	FV Tau/c	10572	3327	<0.008	3.49	<29.82	17.2	M3.5	20	...	...	-0.32	3	30.44	...	5.04	...
393	L1551/IRS 5	7247	10563	<0.003	1.28[i]	<29.32	...	K2	...	...	...	...	...	...	...	...	...
406	HN Tau/c	867	2054	<0.015	0.54	<30.18	18.1	M	89	...	...	...	...	...	...	...	...

NOTES FOR TABLES 1A AND 1B.—Many of the X-ray sources appearing in the tables have two (or three) T Tauri counterparts. Tabulated count rates refer to the X-ray source and have been divided by the number of counterparts to yield the L_x in the last column. Unresolved pairs are: RY Tau/LkCa 21, DH/DI Tau, UX Tau A/B, V710 Tau A/B, GH/V807 Tau, GI/GK Tau, RW Aur A/B, 035120+3154 SW/NE, 035135+2528 NW/SE, 040012+2545 S/N, 040047+2603 W/E, 040142+2150 SW/NE, plus the group HL Tau, XZ Tau, and LkHα 358.

[a] A_V from Strom et al. 1989 (detections) and Cohen & Kuhi 1979 (upper limits).

[b] m_v, spectral types, and EW(Hα) from Herbig & Bell 1988, except for m_v of HBC 382 (Martin et al. 1994) and HBC 404 (Bouvier et al. 1993).

[c] $L_{H\alpha}$ derived from literature data, as described in Paper II.

[d] $L_{25\mu m}$ is the luminosity in the 16–30 μm band, derived from $f_{25\mu m}$ listed by Strom et al. 1989.

[e] Source detected in two different IPC images, free from detector rib occultation. In these cases a maximum likelihood method was used to derive the L_x (and S/N) listed in the table.

[f] A_V not found in literature; the average A_V for other detections has been adopted in the derivation of count-rate to flux conversion factor.

[g] Source detected with the Local method in the broad band.

[h] L_{bol} derived from m_v and bolometric correction.

[i] A_V not found in literature; the average A_V for other upper limits has been adopted in the derivation of count-rate to flux conversion factor.

REFERENCES FOR TABLES 1A AND 1B.—(1) Herbig & Bell 1988; (2) Vrba et al. 1984; (3) Cohen, Emerson & Beichman 1989; (4) Red'kina & Zausaeva 1987; (5) Herbst et al. 1986; (6) Bouvier & Bertout 1989; (7) Rydgren et al. 1985; (8) Bouvier et al. 1986; (9) Cohen & Kuhi 1979; (10) Vrba et al. 1986; (11) Herbst et al. 1987; (12) Herbig 1962; (13) Walter et al. 1988; (14) Walter et al. 1987; (15) Rydgren et al. 1984; (16) Walter 1986; (17) Praderie et al. 1986; (18) Bouvier et al. 1993; (19) Martin et al. 1994.

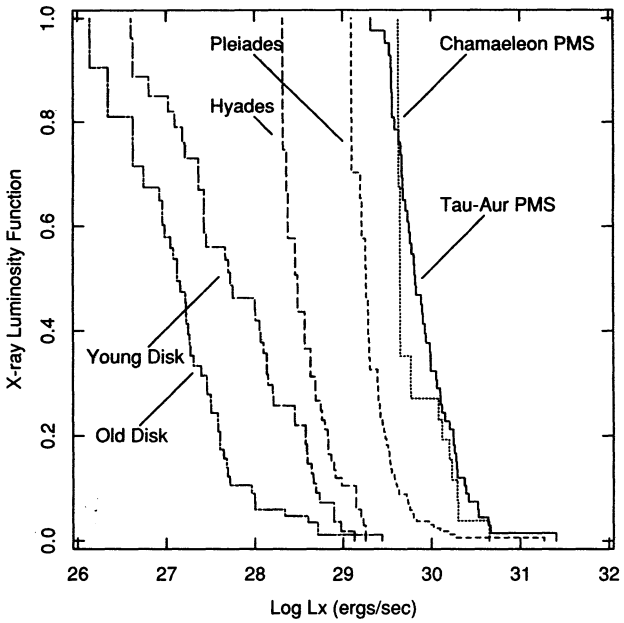

FIG. 4.—X-ray luminosity function of Taurus-Auriga T Tauri stars, compared with those of Chamaeleon stars (Feigelson & Kriss 1989), K-M stars of the Pleiades (Micela et al. 1990), Hyades (Micela et al. 1988), and young and old disk populations (Barbera et al. 1993).

s^{-1}). There are reasons, in any case, to think that the average X-ray luminosity is not far from this value, even for WTTSs, since if we restrict to consider only the WTTSs discovered independent of X-ray observations (V807 Tau, NTTS 042950+1757, NTTS 042916+1751, LkCa 19, and NTTS 041636+2743; Walter et al. 1988; Feigelson & Kriss 1983), we find a median log $L_x = 29.9$.

In Figure 4, we have compared the total sample L_x maximum likelihood distribution with analogous distributions already obtained by various authors for the Chamaeleon star formation region (Feigelson & Kriss 1989), the Pleiades K–M stars (Micela et al. 1990), the Hyades K–M stars (Micela et al. 1988), and the young and old disk K–M stars (Barbera et al. 1993). The fact that in Figure 4 the Taurus-Auriga and Chamaeleon luminosity functions intersect should be not surprising. The low-luminosity region of the Taurus-Auriga luminosity function is populated due to a few deep IPC exposures, which were not available for Chamaeleon stars. The high-L_x tail of the Taurus-Auriga luminosity function is populated by only two stars, which scaled to the smaller Chamaeleon sample size is compatible with zero detected stars at this high L_x value.

We also report in Figure 5 the median X-ray luminosities of these samples as a function of the stellar age. Vertical bars indicate the 16%–84% quantile range of L_x, approximately describing the (1 σ) dispersion for each stellar sample. As is seen in the figure, the range of X-ray luminosities in Taurus-Auriga turns out to be nearly the same as in Chamaeleon. Therefore, our study of Taurus-Auriga PMS stars suggests that the decrease of X-ray luminosity of late-type stars with increasing stellar age can be definitely extended to the PMS phase of evolution, confirming results based on previous work (e.g., Feigelson & Kriss 1989). We find that the range of L_x for stars in stellar formation regions such as Taurus-Auriga is at least two orders of magnitude, hence some parameters other than age have to be invoked in order to explain it.

We should note also that the Chamaeleon region has been recently observed with the *ROSAT* Position Sensitive Proportional Counter (PSPC), and a new estimate of its X-ray luminosity function is now available (Feigelson et al. 1993). The main differences with respect to the IPC luminosity function of Feigelson & Kriss (1989) are its extension toward lower X-ray luminosities and the depletion of part of its high-luminosity tail, as a consequence of the higher sensitivity and spatial resolution of the PSPC, respectively. Indeed, some strong IPC sources were resolved into many weaker components with the *ROSAT* PSPC. Differences in the performances of the two instruments, however, make of dubious validity a direct comparison of IPC and PSPC luminosity functions, as Feigelson et al. (1993) also note. Therefore, although the PSPC luminosity function is undoubtedly a better estimate of the true L_x distribution in Chamaeleon, we have preferred to compare our results with the older IPC data (Feigelson & Kriss 1989) for this star formation region.

3.2. *X-Ray Emission Levels for Different Classes of Stars*

In order to get some insight into the nature of the X-ray emission of our sample stars, we have compared the average X-ray emission levels of subsamples having different properties. Since PMS stars are characterized by optical emission lines and IR excesses, we have examined whether these diagnostics are related to the observed X-ray activity. First, we have separated stars having EW(Hα) greater and less than 10 Å, respectively. The corresponding X-ray luminosity functions for these two subsamples are plotted and compared in Figure 6. To confirm the difference apparent from the figure, we applied a Wilcoxon test (Feigelson & Nelson 1985) to the two distributions and found that the null hypothesis (that they are drawn from the same parent population) is rejected at the 99.67% confidence level.

This result should however be interpreted with caution: as noted in § 2.1, most (~70%) stars having EW(Hα) < 10 Å have

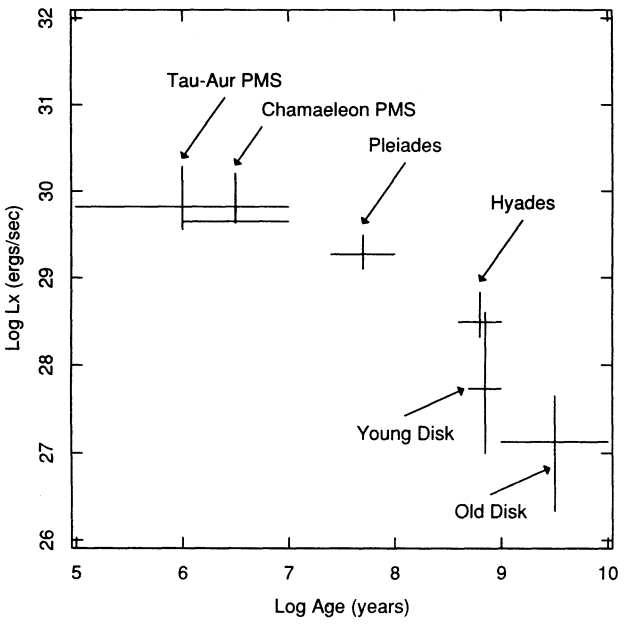

FIG. 5.—X-ray luminosity (median and ± 1 σ values for each distribution) as a function of age, for the same groups of stars as in Fig. 4.

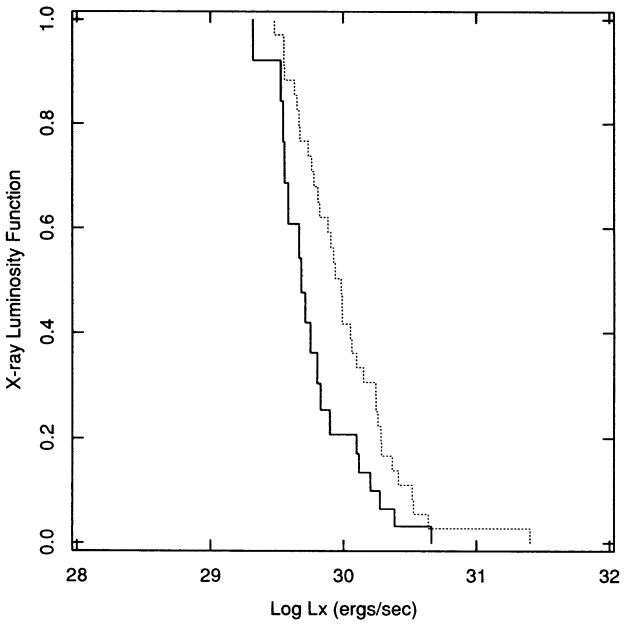

FIG. 6.—X-ray luminosity function for Taurus-Auriga T Tauri stars having EW(Hα) > 10 Å (*solid*) and EW(Hα) < 10 Å (*dotted*).

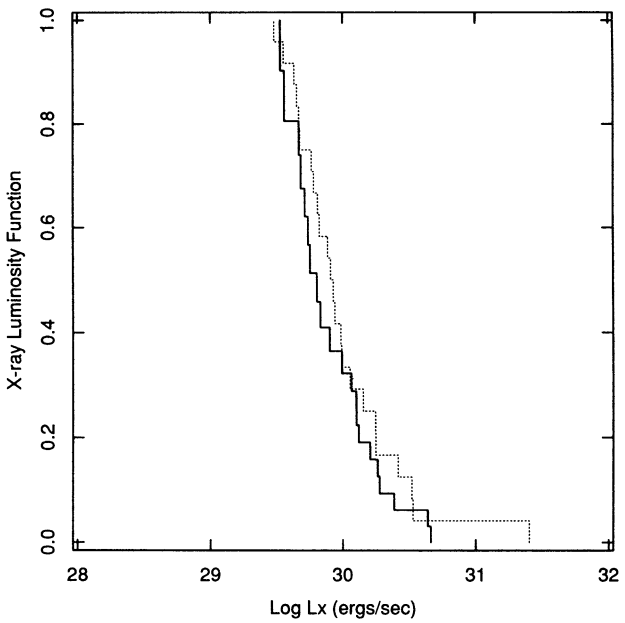

FIG. 7.—X-ray luminosity function for stars detected (*solid*) and not detected (*dotted*) at 25 μm.

just been discovered through X-ray observations, and their X-ray luminosity function might be therefore biased toward high L_x values. In order to reduce this bias, although with the caveat of § 2.1, we considered only the (10) stars both having EW(Hα) < 10 Å and identified as PMS objects independent from their X-ray emission (DI Tau, UX Tau A/B, SU Aur, V710 Tau B, IQ Tau, NTTS 042950+1757, NTTS 042916+1751, LkCa 19, and NTTS 041636+2743): their L_x distribution appears indistinguishable from that of the whole sample with EW(Hα) < 10 Å, possibly indicating that our previous result is not to be biased by the inclusion of X-ray–selected stars. We conclude that stars having EW(Hα) respectively larger and smaller than 10 Å have, on average, different L_x.

We have also evaluated X-ray luminosity functions for CTTSs and WTTSs separated according to their IR emission (Fig. 7). Here we have separated stars which were detected at 25 μm by the satellite *IRAS* (Harris, Clegg, & Hughes 1988; Strom et al. 1989) from those which were not; this amounts to fixing a threshold log $L_{25\,\mu m} = 31.25$ (ergs s^{-1}; emitted in the 16–30 μm band) at the Taurus-Auriga distance (for a limiting observed flux of 0.1 Jy), a value which arises in a natural way, since almost all upper limits on $L_{25\,\mu m}$ lie below it, while all detections are clearly above (cf. Table 1; see also Skrutskie et al. 1990; and Paper II). In this case the two classes only differ at the 62% confidence level, and by choosing the detectability at 12 μm rather than at 25 μm as the separating criterion, the confidence level drops to only 53%; i.e., they are indistinguishable. Therefore, we find that stars with very different far-IR emission exhibit indistinguishable X-ray behavior.

It is worth noting that the two classifications we have made are quite similar to each other, since most stars detected at 25 μm have EW(Hα) > 10 Å (Strom et al. 1989). The different behavior of the average X-ray luminosity as a function of IR emission and Hα equivalent width respectively suggests therefore that we are looking at subtle effects (yet statistically significant). This problem deserves further investigation, also in light of current models of T Tauri stars; it will be examined in Paper II.

4. SUMMARY

We have reanalyzed all available *Einstein* IPC X-ray data on the PMS population of the Taurus-Auriga star formation region in a systematic way, on the basis of REV 1 IPC data. We derive X-ray luminosities and upper limits uniformly for both strong- and weak-line T Tauri populations of the cluster and discuss how representative the studied sample is. Some of our findings are in qualitative agreement with previous studies, confirming them on a more sound statistical basis.

Our main results are:

1. A maximum likelihood X-ray luminosity function has been built, including X-ray–undetected stars, for the whole known PMS population in Taurus-Auriga.

2. The X-ray luminosity distribution of T Tauri stars in Taurus-Auriga allows us to evaluate the median log $L_x \sim 29.7$ (ergs s^{-1}), at least for stars selected independent from their X-ray emission, although higher spatial resolution and a lower detection threshold are required to better constrain the median L_x.

3. The average level of X-ray emission in Taurus-Auriga turns out to follow the trend of decreasing X-ray luminosity with age known for main-sequence young stars, as already found for the T Tauri population of the Chamaeleon star-forming region.

4. Using the Hα equivalent width as a separating criterion, a significant difference is found between the X-ray luminosity distributions of strong- and weak-emission line stars.

5. No significant difference exists between the X-ray luminosity distributions of stars having IR emission at 25 μm respectively higher and lower than a threshold of log $L_{25\,\mu m} = 31.25$ ergs s^{-1} (0.1 Jy).

6. The IPC X-ray spectra of two stars with the highest number of X-ray counts (SU Aur and HD 283572) are well

fitted by Raymond-Smith thermal spectra, with temperatures of 1.1 (1.0–1.5) keV and 1.5 (1.1–2.3) keV, respectively.

This work was inspired by the late G. S. Vaiana, who took part in its early development and without whose contributions this paper might never have been written.

We acknowledge support by the Italian Ministero per la Ricerca Scientifica e Tecnologica, and from Agenzia Spaziale Italiana (F. D., G. M., and S. S.). F. R. H. acknowledges partial support under NASA contract NAS 8-30751. We are grateful to F. Reale, A. Maggio, A. Collura, and H. Tananbaum for useful discussions and comments on this paper, and to D. Randazzo for her help in improving the form of the original manuscript. We are also indebted to the referee and to T. Simon, whose suggestions have allowed us to improve this paper significantly.

REFERENCES

Avni, Y., Soltan, A., Tananbaum, H., & Zamorani, G. 1980, ApJ, 238, 800
Barbera, M., Micela, G., Sciortino, S., Harnden, F. R., Jr., & Rosner, R. 1993, ApJ, 414, 846
Bertout, C. 1989, ARA&A, 27, 351
Bouvier, J., & Bertout, C. 1989, A&A, 211, 99
Bouvier, J., Bertout, C., Benz, W., & Mayor, M. 1986, A&A, 165, 110
Bouvier, J., Cabrit, S., Fernandez, M., Martin, E. L., & Matthews, J. M. 1993, A&A, 272, 176
Caillault, J. P., & Helfand, D. J. 1985, ApJ, 289, 279
Cohen, M., Emerson, J. P., & Beichman, C. A. 1989, ApJ, 339, 455
Cohen, M., & Kuhi, L. V. 1979, ApJS, 41, 743
Damiani, F., & Micela, G. 1995, ApJ, 446, 341 (Paper II)
Eadie, W. T., Drijard, D., James, F. E., Roos, M., & Sadoulet, B. 1971, Statistical Methods in Experimental Physics (Amsterdam: North-Holland)
Favata, F., Barbera, M., Micela, G., & Sciortino, S. 1993, A&A, 277, 428
Feigelson, E. D., Casanova, S., Montmerle, T., & Guibert, J. 1993, ApJ, 416, 623
Feigelson, E. D., & DeCampli, W. M. 1981, ApJ, 243, L89
Feigelson, E. D., Jackson, J. M., Mathieu, R. D., Myers, P. C., & Walter, F. M. 1987, AJ, 94, 1251
Feigelson, E. D., & Kriss, G. A. 1981, ApJ, 248, L35
———. 1983, AJ, 88, 431
———. 1989, ApJ, 338, 262
Feigelson, E. D., & Nelson, P. I. 1985, ApJ, 293, 192
Gahm, G. F. 1980, ApJ, 242, L163
Giacconi, R., et al. 1979, ApJ, 230, 540
Gioia, I. M., Maccacaro, T., Schild, R. E., Wolter, A., Stocke, J., Morris, S., & Henry, J. P. 1990, ApJS, 72, 567
Gorenstein, P. 1975, ApJ, 198, 95
Gorenstein, P., Harnden, F. R., & Fabricant, D. G. 1981, IEEE Nucl. Sci., NS-28, 869
Harnden, F. R., Jr., Fabicant, D. G., Harris, D. E., & Schwartz, J. 1984, Smithsonian Astrophys. Obs. Spec. Rept. 393
Harris, D. E., et al. 1993, The *Einstein Observatory* Catalog of IPC X-Ray Sources, Vol. 1 (NASA TM-108401)
Harris, S., Clegg, P., & Hughes, J. 1988, MNRAS, 235, 441
Hartmann, L., Calvet, N., Avrett, E. H., & Loeser, R. 1990, ApJ, 349, 168
Herbig, G. H. 1962, Adv. Astron. Astrophys., 1, 47
Herbig, G. H., & Rao, N. K. 1972, ApJ, 174, 401
Herbig, G. H., & Bell, K. R. 1988, Third Catalog of Emission-Line Stars of the Orion Population (Lick Obs. Bull. 1111)
Herbig, G. H., Vrba, F. J., & Rydgren, A. E. 1986, AJ, 91, 575
Herbst, W., et al. 1986, ApJ, 310, L71
———. 1987, AJ, 94, 137
Kenyon, S. J., & Hartmann, L. W. 1990, ApJ, 349, 197
Martin, E. L., Rebolo, R., Magazzù, A., & Pavlenko, Ya. V. 1994, A&A, 282, 503
Micela, G., Sciortino, S., Serio, S., Vaiana, G. S., Bookbinder, J., Golub, L., Harnden, F. R., & Rosner, R. 1985, ApJ, 292, 172
Micela, G., Sciortino, S., Vaiana, G. S., Harnden, F. R., Rosner, R., & Schmitt, J. H. M. M. 1990, ApJ, 348, 557
Micela, G., Sciortino, S., Vaiana, G. S., Schmitt, J. H. M. M., Stern, R. A., Harnden, F. R., & Rosner, R. 1988, ApJ, 325, 798
Montmerle, T., Koch-Miramond, L., Falgarone, E., & Grindlay, J. E. 1983, ApJ, 269, 182
Mundt, R., Walter, F. M., Feigelson, E. D., Finkenzeller, U., Herbig, G. H., & Odell, A. P. 1983, ApJ, 269, 229
Praderie, F., Simon, T., Catala, C., & Boesgaard, A. M. 1986, ApJ, 303, 311
Raymond, J. C., & Smith, B. W. 1977, ApJS, 35, 419
Red'kina, N. P., & Zausaeva, O. G. 1987, Astron. Tsirk., 1523, 5
Rosner, R., Golub, L., & Vaiana, G. S. 1985, ARA&A, 23, 413
Rosner, R., & Vaiana, G. S. 1980, in X-Ray Astronomy, ed. G. Setti & R. Giacconi (Dordrecht: Reidel), 129
Rydgren, A. E., Vrba, F. J., Chugainov, P. F., & Shakhovskaya, N. I. 1985, BAAS, 17, 556
Rydgren, A. E., Zak, D. S., Vrba, F. J., Chugainov, P. F., & Zajtseva, G. V. 1984, AJ, 89, 1015
Schmitt, J. H. M. M. 1985, ApJ, 293, 178
Schrijver, C. J., Mewe, R., & Walter, F. M. 1984, A&A, 138, 258
Sciortino, S. 1993, in Physics of Solar and Stellar Coronae, ed. J. Linsky & S. Serio (Dordrecht: Kluwer), 211
Sciortino, S., & Micela, G. 1992, ApJ, 388, 595
Skrutskie, M. F., Dutkevitch, D., Strom, S. E., Edwards, S., Strom, K. M., & Shure, M. A. 1990, AJ, 99, 1187
Stocke, J. T., et al. 1991, ApJS, 76, 813
Strom, K. M., et al. 1990, ApJ, 362, 168
Strom, K. M., & Strom, S. E. 1994, ApJ, 424, 237
Strom, K. M., Strom, S. E., Edwards, S., Cabrit, S., & Skrutskie, M. F. 1989, AJ, 97, 1451
Vaiana, G. S., et al. 1981, ApJ, 245, 163
Vaiana, G. S., Maggio, A., Micela, G., & Sciortino, S. 1992, Mem. Soc. Astron. Italiana, 63, 545
Vrba, F. J., Rydgren, A. E., Chugainov, P. F., Shakovskaya, N. I., & Zak, D. S. 1986, ApJ, 306, 199
Vrba, F. J., Rydgren, A. E., Zak, D. S., Chugainov, P. F., & Shakhovskaya, N. I. 1984, BAAS, 16, 998
Walter, F. M. 1986, ApJ, 306, 573
Walter, F. M., et al. 1987, ApJ, 314, 297
Walter, F. M., Brown, A., Mathieu, R. D., Myers, P. C., & Vrba, F. J. 1988, AJ, 96, 297
Walter, F. M., & Kuhi, L. V. 1981, ApJ, 250, 254
———. 1984, ApJ, 284, 194